# Optimum conditions for electron acceleration using tightly focused laser beams

**Conference Paper** *in* Laser Physics · April 2003

CITATIONS
6

READS
97

**2 authors**, including:

Yousef I Salamin
American University of Sharjah
**104** PUBLICATIONS **2,566** CITATIONS

SEE PROFILE

*Laser Physics, Vol. 13, No. 4, 2003, pp. 407–413.*




# Optimum Conditions for Electron Acceleration Using Tightly Focused Laser Beams

**Y. I. Salamin[1] and C. H. Keitel[2]**

[1] *Physics Department, Birzeit University, P. O. Box 14 - Birzeit, West Bank, Palestine*
e-mail: ysalamin@birzeit.edu

[2] *Theoretische Quantendynamik, Fakultät für Physik, Universität Freiburg, Hermann-Herder-Strasse 3, D-79104 Freiburg, Germany*
e-mail: keitel@physik.uni-freiburg.de

Received September 16, 2002

**Abstract**—We investigate optimum conditions for achieving maximum energy gain when electrons are scattered by tightly focused laser beams. A single-beam configuration and one that employs two beams crossing at an angle are discussed. Solution of the equations of motion is carried out numerically in each case, and the fields are modeled by those of a Gaussian beam to order $\epsilon^5$, where $\epsilon$ is the beam diffraction angle. It is shown that the gain in the GeV range may be obtained when MeV electrons are scattered by petawatt laser beams of a few micron waist radii.

## 1. INTRODUCTION

There has been a revival recently [1–6] of efforts to utilize high-intensity laser beams in the acceleration of free electrons to high energies; a means that aims at potentially replacing the large and costly conventional accelerators. Several schemes were suggested in the past and have been revisited lately in the light of new developments in laser technology [7].

In order to achieve the goal of achieving the highest energy gain, fields of the highest intensity need to be employed. Such fields require focusing over small spatial dimensions and, as a result, develop complicated rapid local phase variations. It is of utmost importance that these variations be understood and correctly modeled if they are to be used efficiently for the purpose of particle acceleration to high energies. We recently demonstrated [4, 5] by using numerical simulations that an electron may gain GeV energy when injected sideways into the focal region of a 10 petawatt (PW) laser beam. The fields were modeled by using those of a Gaussian beam focused to a waist radius of a few microns and in whose description terms of order $\epsilon^5$, where $\epsilon$ is the diffraction angle (see Fig. 1), have been retained.

It turns out that the field strengths, and hence the ultimate energy gained by the electron from interaction with them, are sensitive to the above-mentioned local phase variations. In a sense, one needs to look for an optimal set of initial conditions that would allow the electron to sample regions around the beam's focal spot where the fields are likely to impart the strongest series of violent impulses to it and cause it to escape with a maximum energy gain. This is not a simple matter, for there is quite a number of parameters to be investigated and discussed in the present paper that must be dealt with which compete with one another in a very complicated way.

We describe the fields of a tightly focused beam in Section 2 and review the equations of motion and outline their solution in Section 3. In Section 4 the acceleration of a single electron by a single laser beam is investigated. Acceleration in two crossed beams then follows in Section 5. Some concluding remarks are finally given in Section 6.

## 2. THE LASER FIELDS

Most of the material in this section may be found elsewhere [4, 5]. It is given here in the desire to make the present paper as self-contained as possible. The geometry of our Gaussian beam is shown in Fig. 1. The beam axis is taken along $z$, with its propagation direction along $+z$ and *stationary* focus at the origin of coordinates O. The beam cross section at the focus is a circle of radius $w_0$; the cross section normal to the beam axis and at an arbitrary $z$ is also circular with radius $w(z)$ =

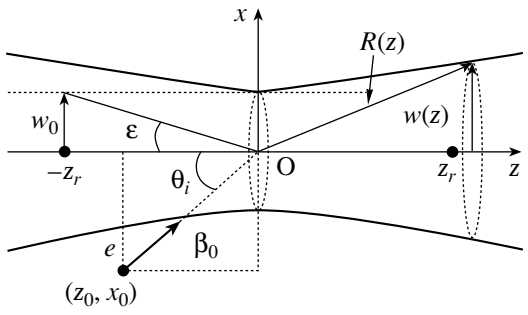


**Fig. 1.** Schematic diagram of the laser accelerator configuration. The electron $e$, with initial scaled speed $\beta_0$, is injected sideways at an angle $\theta_i$ to the $z$ axis, with the latter serving as the direction of beam propagation.

$w_0\sqrt{1+(z/z_r)^2}$. Furthermore, $z_r = kw_0^2/2$ is the Rayleigh length and $\epsilon = w_0/z_r$ is the diffraction angle. Now, with $\xi = x/w_0$, $v = y/w_0$, and $\zeta = z/z_r$, the electric components of the laser field associated with such a beam are [5, 8–10]

$$E_x = E\left\{S_0 + \epsilon^2\left[\xi^2 S_2 - \frac{\rho^4 S_3}{4}\right] + \epsilon^4\left[\frac{S_2}{8} - \frac{\rho^2 S_3}{4} - \frac{\rho^2(\rho^2 - 16\xi^2)S_4}{16} - \frac{\rho^4(\rho^2 + 2\xi^2)S_5}{8} + \frac{\rho^8 S_6}{32}\right]\right\}, \quad (1)$$

$$E_y = E\xi v\left\{\epsilon^2[S_2] + \epsilon^4\left[\rho^2 S_4 - \frac{\rho^4 S_5}{4}\right]\right\}, \quad (2)$$

$$E_z = E\xi\left\{\epsilon[C_1] + \epsilon^3\left[-\frac{C_2}{2} + \rho^2 C_3 - \frac{\rho^4 C_4}{4}\right] + \epsilon^5\left[-\frac{3C_3}{8} - \frac{3\rho^2 C_4}{8} + \frac{17\rho^4 C_5}{16} - \frac{3\rho^6 C_6}{8} + \frac{\rho^8 C_7}{32}\right]\right\}. \quad (3)$$

Similarly, the magnetic field components are given by

$$B_x = 0, \quad (4)$$

$$B_y = E\left\{S_0 + \epsilon^2\left[\frac{\rho^2 S_2}{2} - \frac{\rho^4 S_3}{4}\right] + \epsilon^4\left[-\frac{S_2}{8} + \frac{\rho^2 S_3}{4} + \frac{5\rho^4 S_4}{16} - \frac{\rho^6 S_5}{4} + \frac{\rho^8 S_6}{32}\right]\right\}, \quad (5)$$

$$B_z = Ev\left\{\epsilon[C_1] + \epsilon^3\left[\frac{C_2}{2} + \frac{\rho^2 C_3}{2} - \frac{\rho^4 C_4}{4}\right] + \epsilon^5\left[\frac{3C_3}{8} + \frac{3\rho^2 C_4}{8} + \frac{3\rho^4 C_5}{16} - \frac{\rho^6 C_6}{4} + \frac{\rho^8 C_7}{32}\right]\right\}. \quad (6)$$

In Eqs. (1)–(6), we have taken

$$E = E_0\frac{w_0}{w}g(\eta)\exp\left[-\frac{r^2}{w^2}\right], \quad (7)$$

$$S_n = \left(\frac{w_0}{w}\right)^n \sin(\psi + n\psi_G), \quad (8)$$

$$C_n = \left(\frac{w_0}{w}\right)^n \cos(\psi + n\psi_G). \quad (9)$$

Furthermore, $k = \omega/c$, $kA_0 = E_0$, $r^2 = x^2 + y^2$, and $\rho = r/w_0$. For more details on the calculation leading to Eqs. (1)–(6), see the appendix to [5]. These equations were derived from a vector potential polarized along $x$ having an amplitude $A_0$ and a frequency $\omega$. The remaining symbols in Eqs. (1)–(9) have the following definitions:

$$\psi = \psi_0 + \psi_P - \psi_R + \psi_G, \quad (10)$$

$$\psi_P = \omega t - kz, \quad (11)$$

$$\psi_G = \tan^{-1}\zeta, \quad (12)$$

$$\psi_R = \frac{kr^2}{2R}, \quad (13)$$

$$R(z) = z + \frac{z_r^2}{z}. \quad (14)$$

Note that $\psi_0$ is a constant phase, $\psi_P$ is the plane wave phase, $\psi_G$ is the Guoy phase associated with the fact that a Gaussian beam undergoes a total phase change of $\pi$ as $z$ changes from $-\infty$ to $+\infty$, $\psi_R$ is the phase associated with the curvature of the wave fronts, and that $R(z)$ is the radius of curvature of a wavefront intersecting the beam axis at the coordinate $z$. The fields given above satisfy Maxwell's equations $\nabla \cdot \mathbf{E} = 0 = \nabla \cdot \mathbf{B}$, plus terms of order $\epsilon^6$ [5].

A laser system is often characterized by its output power $P$. For the fields given by Eqs. (1)–(6), the power may be calculated by integrating the time-averaged Poynting vector over a plane through the beam focus and perpendicular to its axis. Dropping terms of order $\epsilon^6$ and smaller in the result, one gets

$$P[TW] = \frac{\pi w_0^2}{2} I_0\left[1 + \frac{\epsilon^2}{4} + \frac{\epsilon^4}{8}\right] \approx 0.0216\left(\frac{qw_0}{\lambda}\right)^2\left[1 + \frac{\epsilon^2}{4} + \frac{\epsilon^4}{8}\right], \quad (15)$$

where $I_0 = I(0, 0, 0) = cE_0^2/8\pi$ is the peak intensity (at the focus). Equation (15) clearly shows that, for a fixed laser output power, the peak intensity is inversely proportional to the square of the beam waist radius or, equivalently, the dimensionless intensity parameter $q = eE_0/(mc\omega)$ is inversely proportional to $w_0$. Note that Gaussian cgs units are used throughout this work.

## 3. THE EQUATIONS OF MOTION

Let the electron have mass $m$ and charge $-e$. Its dynamics, subsequent to injection into the focus of the beam in the manner schematically depicted in Fig. 1, may then be investigated by numerically solving the relativistic equations of motion

$$\frac{d\mathbf{p}}{dt} = -e(\mathbf{E} + \boldsymbol{\beta} \times \mathbf{B}), \quad \frac{d\mathscr{E}}{dt} = -ec\boldsymbol{\beta} \cdot \mathbf{E}. \quad (16)$$

In Eq. (16), $\mathbf{p} = \gamma mc\boldsymbol{\beta}$ is the relativistic momentum of the electron and $\mathscr{E} = \gamma mc^2$ is its energy, where $\boldsymbol{\beta}$ is the

velocity vector normalized by the speed of light and $\gamma = (1 - \beta^2)^{-1/2}$ is the Lorentz factor.

With the full fields (1)–(6), only numerical integration is likely to produce tangible results. To look for analytic solutions is quite hopeless. Neither will perturbation techniques [11] yield any meaningful results; in fact, such techniques break down altogether in the regime of relativistic intensities we are interested in ($q \gg 1$).

Quite a few interesting aspects of the electron dynamics may be investigated based on the solutions of Eqs. (16). Elsewhere [4, 5], actual trajectories, momenta, and energy gains of electrons accelerated by a single laser beam, as well as by two crossed beams, have been studied in detail. We have found that the electron receives a series of violent impulses from the fields and ends up gaining energy in the GeV range. Our main interest in this paper is in the energy gain $G(t)$ defined by

$$G(t) = [\gamma(t) - \gamma_0]mc^2 \tag{17}$$

and in ways to render it a maximum through correctly choosing the laser parameters and electron initial conditions. We do this for two configurations: a single beam arrangement and one that involves two identical beams crossing at some angle.

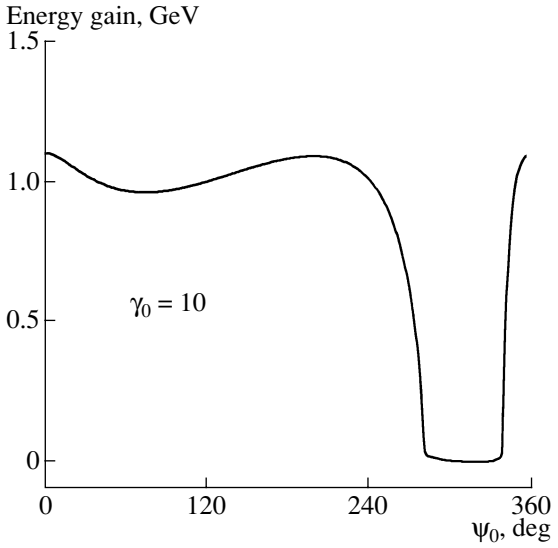


**Fig. 2.** Energy gain vs. the constant phase $\psi_0$ corresponding to two injection energies but the same injection angle $\theta_i = 10°$ and $z_0 = -5$ mm. The laser parameters are as follows: power $P = 10$ PW, wavelength $\lambda = 1$ μm, and waist radius $w_0 = 10$ μm. Injection is into the laser focus and the interaction time, starting from injection at $t = 0$, is equivalent to $\Delta\eta = 10\,650\pi$, with $\eta = \omega(t - z/c)$.

## 4. ACCELERATION BY A SINGLE LASER BEAM

Without any loss of generality, we will consider initial electron motion in the *xz* plane only. In this plane, the field components $E_y$ and $B_z$ vanish identically ($y = 0$). Subsequent motion will therefore be governed by the two force components

$$F_x = -e(E_x - \beta_z B_y), \tag{18}$$

$$F_z = -e(E_z + \beta_x B_y). \tag{19}$$

Thus, for such an admittedly idealized initial condition, no motion out of the *xz* plane will be possible.

What happens when an electron is injected sideways (see Fig. 1) into the focal region of a laser beam? The answer to this question, roughly speaking, is that the outcome depends on how energetic the electron is upon injection. A slow electron, with an injection energy $\mathcal{E}_0 = \gamma_0 mc^2$ much smaller than the ponderomotive potential energy of the laser $U_p = (eE_0)^2/4m\omega^2$, will be reflected. One that is injected with $\mathcal{E}_0 \gg U_p$ will penetrate the beam and show up on the other side, i.e., will be transmitted. In-between these two extremes, the electron may get captured and violently accelerated.

The picture, in fact, is much more detailed than this and the criteria that distinguish between the phenomena of reflection, capture, and transmission can not be made any sharper, due in large measure to the complicated local phase variations of the fields, in space as well as in time. Our previous work has shown that gain is largest in capture cases. Reflection and transmission result mostly in little gain, or even loss, but may be accompanied by occasional high gains. In all our calculations in this section, the (plane-wave) phase $\eta = \omega(t - z/c)$ is used as the integration variable. This choice ensures stability and efficiency of the numerics. In this section, the gain is reported as $G(\eta_f)$, where $\eta_f = 650\pi$ and where $\eta_0 = -\omega z_0/c$.

Suppose that we have a laser system of output power $P = 10$ PW, wavelength $\lambda = 1$ μm, and beam waist radius $w_0 = 10$ μm. Consider an electron injected right into the focus at an angle $\theta_i = 10°$ from a point in the *xz* plane with $z_0 = -5$ mm. The fields such an electron will encounter at all space–time points of its trajectory will be determined by the constant phase $\psi_0$, this being embedded in the field equations. Also, the size of $\gamma_0$ will determine the extent to which the electron penetrates the beam and, hence, which space–time points it will sample. In Fig. 2, we show the gain corresponding to $\gamma_0 = 10$ (injection kinetic energy ~4.6 MeV) as a function of the constant phase $\psi_0$. Two main features specific to the chosen set of parameters are demonstrated in this figure. The gain is maximum at $\psi_0 = 3°$ and is a negligible minimum over a range of $\psi_0$ values extending roughly from 280°–340°.

Next, we adopt the value of $\psi_0$ that renders the gain in Fig. 2 a maximum, namely, 3°, and calculate the gain as a function of the injection angle $\theta_i$. We show this in Fig. 3, where the local field phase variations are reflected in the highly oscillating gain at the injection angle. It should be borne in mind that these are not necessarily the variations along the line defined by $\theta_i = 10°$, for we have seen elsewhere [4, 5] that the electron actu-

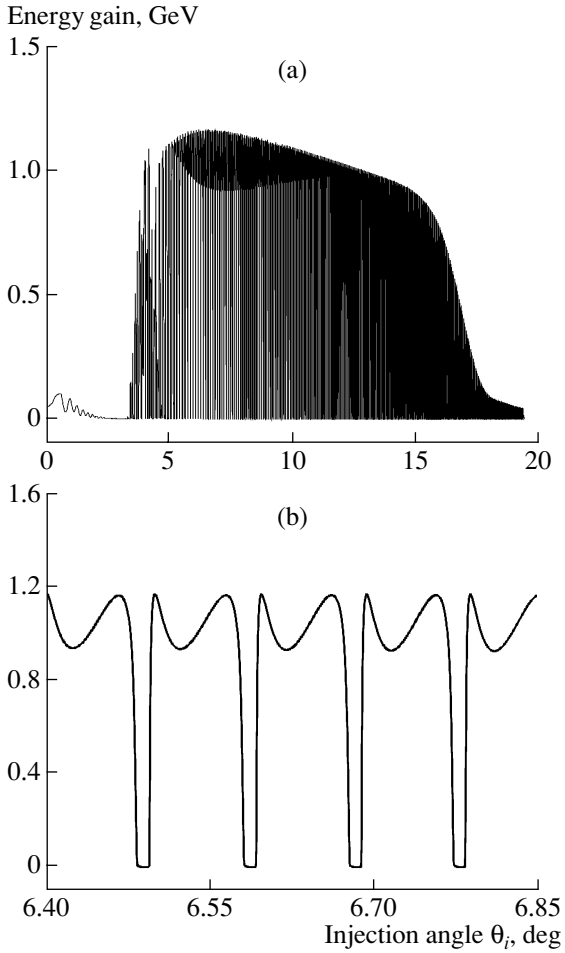


**Fig. 3.** Energy gain vs. the injection angle $\theta_i$ corresponding to a scaled injection energy $\gamma_0 = 10$ and an initial phase constant $\psi_0 = 3°$. The remaining parameters and initial conditions are the same as in Fig. 2. In (b), we only zoom onto a small portion of (a).

ally suffers multiple scatterings by the field, may change direction quite violently, and traverse regions on either side of this line and too far away from it. The magnitude of the gain is, in any case, a measure of how strong the field is locally. The examples presented thus far have been for electrons injected into the beam focus. Next, we fix the injection angle at the value that makes the gain a maximum in Fig. 3, fix $z_0$ at $-5$ mm, and vary $x_0$ by aiming the injected particle at a point $P$ (see Fig. 4 for the schematic) on the beam axis at a distance $s$ away from the focus, to the left ($s < 0$) as well as to the right ($s > 0$). Variation of $x_0$ in this way amounts to looking at a collimated beam of electrons of varying transverse cross section with the space-charge effects entirely neglected. Such a beam will have a diameter $d = |x_0 - \bar{x}_0|\cos\theta_i$, where $\bar{x}_0$ is the value of $x_0$ corresponding to $s = -z_r$. In Fig. 5, we show the gain against $d$ and $s$, with the latter expressed in units of the Rayleigh length $z_r$. Note that injection into the focus ($s = 0$)

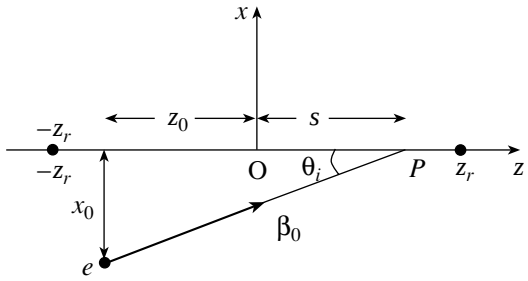


**Fig. 4.** A schematic diagram of electron injection into points on both sides of the beam focus. In this configuration, the initial position coordinates are related via $x_0 = -(s - z_0)\tan\theta_i$, with $s$ positive, negative, or zero.

is not the only case leading to substantial gain. The gain, however, drops markedly if one injects the electron beyond one Rayleigh length on either side of the focal spot, where the fields fall in strength and the intensity drops below 1/2 of its maximum value at focus.

We may view Fig. 5b as giving the gain of many electrons in a beam possessing a circular cross section of diameter $d$. With this view, the following interpretation may not be too far-fetched. For a beam of diameter ~71 μm, its central axis ($d \sim 35.5$ μm) is aimed at the laser beam focus ($s = 0$). Electrons close to the electron beam axis gain the most, while those far away interact with the weak field parts of the laser beam and gain the least amount of energy.

We conclude this section by emphasizing that the cases that lead to the highest energy gain are those in which the electron gets captured by the laser beam. Although it quickly moves *downstream* to the low-intensity parts of the beam far away from the focus, its extraction poses a problem. The use of a mirror to deflect the laser beam and allow the electrons to escape through a hole and the use of a DC magnetic field to deflect the electrons out of the beam have recently been suggested [4, 14].

## 5. ACCELERATION BY TWO TIGHTLY FOCUSED LASER BEAMS

The role played by the magnetic force in the acceleration process of the previous section may easily be appreciated by considering Eqs. (18) and (19). The question then arises as to whether the addition of a second identical laser beam, with its axis oriented at the same angle $\theta_i$ relative to the particle injection direction (see Fig. 6 for the schematic and coordinate system), will result in better gain [3, 12, 13]. The gain in this case depends upon the particulars of the configuration (orientation of the field components of one beam relative to the corresponding components of the other, for example), in addition to depending on the initial conditions and beam parameters. The fields from the two beams interfere. As a result, spots around the common

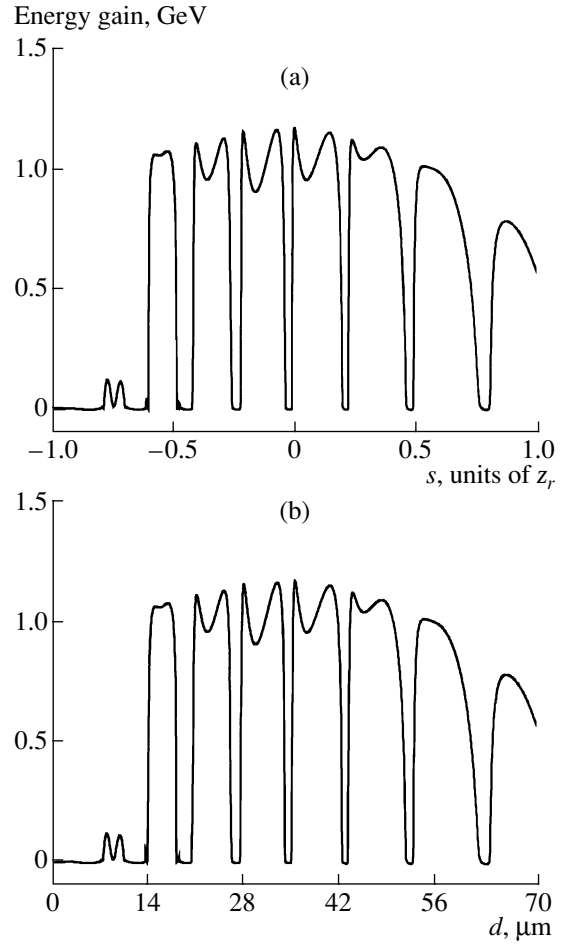


**Fig. 5.** (a) Energy gain when injection is into points on both sides of the beam focus vs. the separation distance $s$ along $z$ from that focus. (b) Gain vs. the equivalent electron beam diameter $d$. See text for explanation.

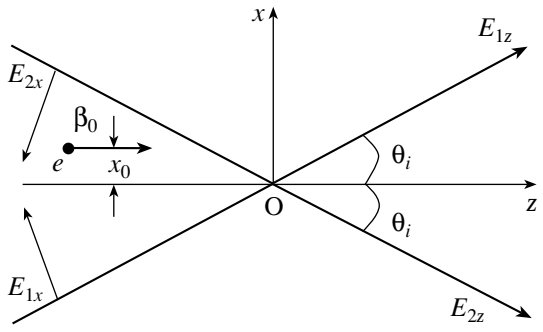


**Fig. 6.** A schematic diagram of electron injection into the region of overlap of two identical laser beams. Note that the coordinate axes of the individual beams are not marked explicitly. The understanding here, and elsewhere, is that $E_{1x}$ points in the direction of $+x_1$, $E_{2z}$ points in the direction of $+z_2$, and so on.

focus will form, at any instant of time, over which the field strength will be enhanced (constructive interference) while it becomes weakened elsewhere (destructive interference).

The advantage of such an arrangement over the single-beam configuration is that the accelerated electrons may escape with the gained energy unaided. They may get accelerated without being captured by either beam, especially in the case of axial injection. The arrangement, as described below, does not require the presence of boundaries, a medium, or additional deflecting mirrors.

In Fig. 6, two identical beams are used with the electron injected parallel to the line through the point of intersection of their axes and at equal angles $\theta_i$ relative to each one. Only the $x$ and $z$ components of the electric fields are shown; the directions of the remaining electric and magnetic field components can be determined by using the right-hand rule. Upon close inspection, one finds that (with $E_{1x}$ standing for the electric field component of beam 1 along $x_1$, $B_{2z}$ representing the magnetic field component of beam 2 along $z_2$, and so forth)

$$E_x = (E_{1x} - E_{2x})\cos\theta_i + (E_{1z} - E_{2z})\sin\theta_i, \quad (20)$$

$$E_y = (E_{1y} - E_{2y}), \quad (21)$$

$$E_z = -(E_{1x} + E_{2x})\sin\theta_i + (E_{1z} + E_{2z})\cos\theta_i, \quad (22)$$

$$B_x = (B_{1z} - B_{2z})\sin\theta_i, \quad (23)$$

$$B_y = (B_{1y} - B_{2y}), \quad (24)$$

$$B_z = (B_{1z} + B_{2z})\cos\theta_i. \quad (25)$$

The three sets of coordinates, on the other hand, transform amongst each other through

$$x_1 = x\cos\theta_i - z\sin\theta_i, \quad (26)$$

$$y_1 = y, \quad (27)$$

$$z_1 = x\sin\theta_i + z\cos\theta_i, \quad (28)$$

$$x_2 = -x\cos\theta_i - z\sin\theta_i, \quad (29)$$

$$y_2 = -y, \quad (30)$$

$$z_2 = -x\sin\theta_i + z\cos\theta_i. \quad (31)$$

Note that $E_x$, $E_y$, $B_x$, and $B_y$ vanish identically for all points on the $z$ axis at all times. Hence, an electron that is injected perfectly axially (along $+z$, $x_0 = 0$) will be subject to a single force component, namely, $F_z = -eE_z$, and its trajectory will be a perfect straight line.

If the phase variations of $E_x$ along the trajectory favor acceleration, then the electron will gain energy. Off-axis injection will obviously be different. Elsewhere on the $xz$ plane, $B_y = 0$ and, hence, injection within that plane, but still parallel to $z$, will result in a two-dimensional trajectory. All remaining possibilities will generally lead to three-dimensional motion.

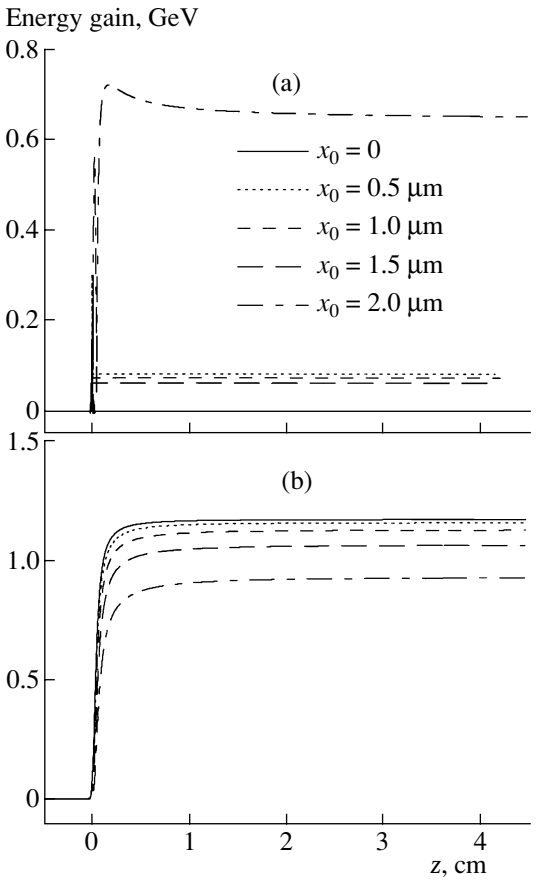


**Fig. 7.** (a) Electron energy gain vs. the forward (axial) distance $z$ and corresponding to several values of off-axis injection distances $x_0$ as a result of interaction with two identical beams. The injection energy is $\gamma_0 = 10$, the crossing half-angle is $\theta_i = 6.5°$, $z_0 = -5$ mm, and the initial phase constant $\psi_0 = 3°$. The remaining parameters and initial conditions are the same as in Fig. 2. (b) Same as (a) but with beam 2 (see Fig. 6) switched off. In both cases, the integration has been carried out over a time equivalent to $5 \times 10^4$ laser periods.

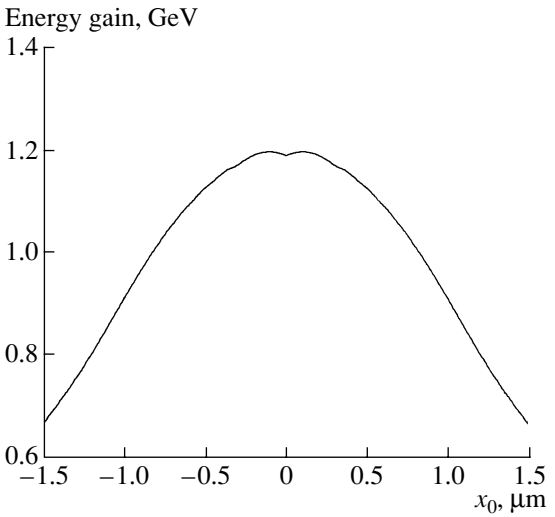


**Fig. 8.** Electron energy gain vs. the off-axis injection distance $x_0$ as a result of interaction with two identical beams. The injection energy is $\gamma_0 = 10$, the crossing half-angle is $\theta_i = 6.5°$, $z_0 = -5$ μm, and the initial phase constant $\psi_0 = 3°$. The remaining parameters and initial conditions are the same as in Fig. 2. The integration has been carried out over a time equivalent to $10^4$ laser periods.

The results presented in Figs. 7 and 8 are also based on solving Eqs. (16) numerically for fields (20)–(25). Real time $t$ is used as the integration variable, and motion of the electron is followed over a time equivalent to 50000 T, where $T = \lambda/c$ is one laser period.

Although a basis for comparison is not really legitimate, because the sets of fields differ drastically, we note that the resulting gains in the double-beam configuration, shown in Fig. 7a, are obviously too small compared to those of the single-beam case, shown in Fig. 7b. Generalization of this result is also baseless. To achieve better gain in the double-beam configuration, one needs to look for a different set of laser and configuration parameters and electron initial conditions. As an example, we show in Fig. 8 results from a more efficient calculation. Figure 8 shows substantial gain when initial conditions that may be tricky to meet are adopted, namely, when $z_0$ is approximately a few microns and we have an injection energy of a few MeV [5]. The assumption here is that the electron is incident from the left with an energy that allows it to penetrate to within 5 μm from the common focus and still meet the stipulated initial condition on velocity.

The main reason behind the low gain in the two-beam configuration is the vanishing of $B_y$ in the $xz$ plane. It has also been found elsewhere [5] that a gain of about 2 GeV may result for beams crossing at a half angle $\theta_i \sim 3.2°$, which is already less than half of the angle used in the examples above. A smaller angle allows for a larger overlap of the two beams and, hence, more interaction time for the *temporarily* captured electron.

We conclude this section by noting that Fig. 8 may actually be viewed as resulting from the scattering of a beam of electrons 3 μm in diameter whose central axis is aimed at the common focus and along $+z$. Electrons close to the electron beam axis gain the most energy, as is also demonstrated in the single-beam results in Fig. 5. Such electrons sample points in space where the fields are maximally intense.

## 6. CONCLUSIONS

We have demonstrated that GeV energies may be gained by an electron injected sideways into, and around, the focal point of a tightly focused laser beam. Conditions to maximize the gain have been investigated that correspond to a predetermined arbitrary subset of laser parameters and initial conditions on the electron

injection. Then, the configuration employing two identical beams crossing at some angle was studied using most of the single-beam parameters and initial conditions. The gain found in this case did not match the maximum obtained in the single-beam case due to the interference effects (which were apparently destructive in the examples we looked at) that result from superposition of the two beams. It does not necessarily follow that the electron cannot achieve a GeV gain in the double-beam arrangement [5]. To the contrary, more energies could be gained if the electron samples regions around the common beam focus where constructive interference of the fields takes place. In general, this type of calculation is quite time-consuming, the more so in the double-beam case than in the single-beam configuration. We have found that the injection energy needs to be large enough to allow the electron to penetrate to the high-intensity points near the common focus of the two beams. Otherwise, multiple reflections would occur and slow the electron down instead of accelerating it.

## ACKNOWLEDGMENTS

YIS gratefully acknowledges support from the German Alexander von Humboldt Stiftung program. CHK is funded by the German Science Foundation (Nachwuchs-gruppe within SFB 276).

## REFERENCES

1. Wang, J.X. *et al.*, 1998, *Phys. Rev. E*, **58**, 6575; Zhu, L.J., Ho, Y.K., Wang, J.X., and Feng, L., 1999, *J. Phys. B*, **32**, 939; Kong, Q. *et al.*, 2000, *Phys. Rev. E*, **61**, 1981; Cheng, Y. and Xu, Z.Z., 1999, *Appl. Phys. Lett.*, **74**, 2116; Wang, P.X. *et al.*, 2001, *Appl. Phys. Lett.*, **78**, 2253.
2. Salamin, Y.I. and Faisal, F.H.M., 2000, *Phys. Rev. A*, **61**, 043801; Salamin, Y.I., Faisal, F.H.M., and Keitel, C.H., 2000, *Phys. Rev. A*, **62**, 053809; Salamin, Y.I. and Keitel, C.H., 2000, *J. Phys. B*, **33**, 5057.
3. Salamin, Y.I. and Keitel, C.H., 2000, *Appl. Phys. Lett.*, **77**, 1082.
4. Salamin, Y.I. and Keitel, C.H., 2002, *Phys. Rev. Lett.*, **88**, 095005.
5. Salamin, Y.I., Mocken, G.R., and Keitel, C.H. 2002, *Phys. Rev.* ST-Accel. Beams **5**, 101301; ibid, 2003, *Phys. Rev.* E **67**, 016501.
6. Bucksbaum, P.H., Bashkansky, M., and McIlrath, T.J., 1987, *Phys. Rev. Lett.*, **58**, 349; Moore, C.I., Knauer, J.P., and Meyerhofer, D.D., 1995, *Phys. Rev. Lett.*, **74**, 2439; Malka, G. and Miquel, J.L., 1996, *Phys. Rev. Lett.*, **77**, 75; Malka, G., LeFebvre, E., and Miquel, J.L., 1997, *Phys. Rev. Lett.*, **78**, 3314; McDonald, K., 1998, *Phys. Rev. Lett.*, **80**, 1350; Mora, P. and Quesnel, B., 1998, *Phys. Rev. Lett.*, **80**, 1351.
7. Perry, M.D. *et al.*, 1999, *Opt. Lett.*, **24**, 160; Andruszkow, J. *et al.*, 2000, *Phys. Rev. Lett.*, **85**, 3825; Stöhlker, Th. *et al.*, 2001, *Phys. Rev. Lett.*, **86**, 983; Drescher, M. *et al.*, 2001, *Sci. Express*, 1058561.
8. Davis, L.W., 1979, *Phys. Rev. A*, **19**, 1177.
9. Barton, J.P. and Alexander, D.R., 1989, *J. Appl. Phys.*, **66**, 2800.
10. McDonald, K.T., www.hep.princeton.edu/~mcdonald/accel/gaussian.ps and gaussian2.ps.
11. Apollonov, V.V., Artemiev, A.I., Kalachev, Yu.L., Prokhorov, A.M., and Fedorov, M.V., 1988, *JETP Lett.*, **44**, 91; Apollonov, V.V., Artemiev, A.I., Kalachev, Yu.L., Suzdaltsev, A.G., Prokhorov, A.M., and Fedorov, M.V., 1990, *Sov. Phys. JETP*, **70**, 846; Apollonov, V.V., Suzdaltsev, A.G., and Fedorov, M.V., 1991, *Laser Phys.*, **1**, 662; Apollonov, V.V., Fedorov, M.V., Prokhorov, A.M., and Suzdaltsev, A.G., 1992, *IEEE J. Quantum Electron.*, **28**, 265.
12. Esarey, E., Sprangle, P., and Krall, J., 1995, *Phys. Rev. E*, **52**, 5443.
13. Huang, Y.C., Zheng, D., Tulloch, W.M., and Beyer, R.L., 1996, *Appl. Phys. Lett.*, **68**, 753; Huang, Y.C. and Beyer, R.L., 1996, *Appl. Phys. Lett.*, **69**, 2175; Huang, Y.C. and Beyer, R.L., 1998, *Nucl. Instrum. Methods Phys. Res. A*, **407**, 316; 1998, *Rev. Sci. Instrum.* **69**, 2629.
14. Hirshfield, J.L. and Wang, C., 2000, *Phys. Rev. E*, **61**, 7252.